Physical Communication 38 (2020) 100910

Contents lists available at ScienceDirect

Physical Communication

journal homepage: www.elsevier.com/locate/phycom

Full length article

Toward emergency rescue: A template-matching-based orientation algorithm using human occlusion error model

Jiawang Wan [a,b,1], Cheng Xu [a,b,c,d,*,1], Xiaotong Zhang [a,b,c,*], Jie He [a,b,c,d], Shihong Duan [a]

[a] School of Computer and Communication Engineering, University of Science and Technology Beijing, China
[b] Shunde Graduate School, University of Science and Technology Beijing, China
[c] Beijing Key Laboratory of Knowledge Engineering for Materials Science, China
[d] Institute of Artificial Intelligence, University of Science and Technology Beijing, Beijing, China

ARTICLE INFO

Article history:
Received 31 May 2019
Received in revised form 25 October 2019
Accepted 25 October 2019
Available online 1 November 2019

Keywords:
Emergency search and rescue
Orientation
Human body occlusion
Template matching

ABSTRACT

Position information is one of the most important properties of an object. In emergency rescue scenarios, barely infrastructure could be deployed in advance, thus traditional positioning technologies are difficult to meet the special needs. We proposed a rotating locator-based orientation method using template matching to obtain the relative positional relationship between the searcher and the trapped. It can help the searcher determine the relative direction to the trapped efficiently. In order to improve the accuracy of orientation, two basic methods are proposed. Firstly, we took the effects of human body occlusion into consideration, and built a corresponding ranging error model. Then, we proposed a template-matching-based algorithm with dividing the matching process into two stages, namely Global Matching and Local Matching. On the one hand, we compared proposed template-matching-based orientation algorithm (TMOA) with other two typical template-matching algorithms. The average angle error of TMOA is 9 degrees, which showed more accurate results than others. On the other hand, to verify the validity of human occlusion error model (HOEM), we executed all three template-matching algorithms improved by HOEM. The average angle error of TMOA improved by HOEM is 4 degrees. Other two algorithms are also more superior under the applying of HOEM.

1. Introduction

In the last decades, indoor positioning has received extensive attentions in various fields, especially emergency rescue in complex building environments [1]. In case of emergencies [2,3], such as the rescue of trapped firefighters or miners, the finding of lost elderly in nursing homes, the searchers need to find the location of the trapped timely and effectively, in order to avoid tragedies.

Many techniques have been considered to solve this problem. Global Positioning System (GPS) [4] has been widely used in outdoor navigation, but it does not work well in indoor conditions due to its weak signal blocked by density building materials. Traditional Radio Frequency Identification (RFID) based positioning [5] is an alternative method, such as received signal strength (RSS) [6], time of arrival (TOA) [7] and time difference of arrival (TDOA) [8]. However, external infrastructure needs to be deployed in advance, which might not be satisfied in emergency rescue scenarios [9,10]. Inertial navigation system (INS) has been used in many commercial products [11] due to its high accuracy and convenience. However, it faces the problems of accumulative error and drifting [12], which to a great extent limits its applications. Above all, existing positioning technologies are difficult to meet the special need of emergency search and rescue.

All above mentioned methods view the rescue process as an absolute positioning problem. However, in order to locate the trapped timely and effectively, search and rescue could be quickly performed by obtaining relative position information between the trapped and the rescuer, instead of absolute coordinates. The authors have previously proposed a method for relative positioning in complex environments and build a commercial locator device for the firefighter rescue applications [13]. It can serve as the basis of this paper.

As shown in Fig. 1, an in-building fire rescue scenario is described. The search and rescue process is divided into two phases: (1) *Altitude Search*: the searcher goes to the same layer of the alarm firefighter, according to the relative height difference; (2) *Horizontal Search*: The searcher uses his own locator to measure distance and RSS with the alarm locator in each possible direction when he needs to select path, and then determine the ahead

* Correspondence to: No. 30, Xueyuan Rd., Haidian Dist., Beijing 100083, PR China.
E-mail addresses: xucheng@ustb.edu.cn (C. Xu), zxt@ies.ustb.edu.cn (X. Zhang).

[1] Jiawang Wan and Cheng Xu are co-first authors and contributed equally to this work.

https://doi.org/10.1016/j.phycom.2019.100910
1874-4907/

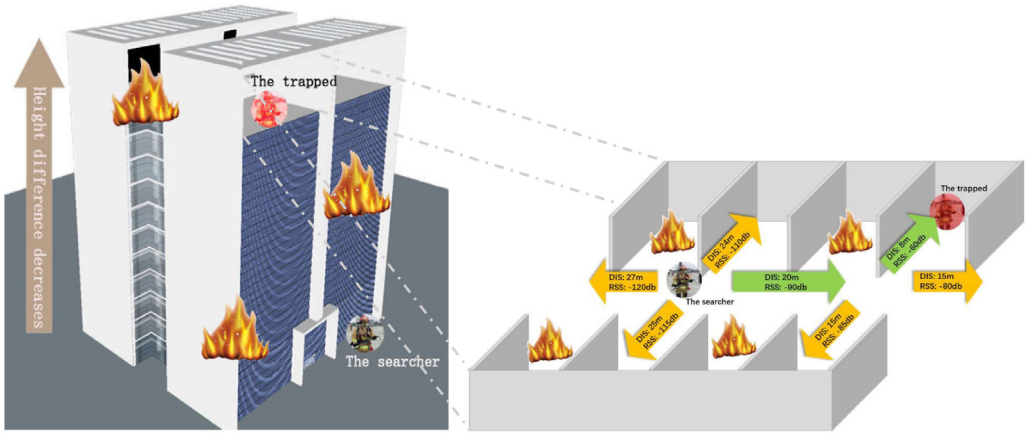

(1) Altitude Search: The searcher goes to the same layer of the trapped, according to the relative height difference.

(2) Horizontal Search: The searcher uses his own locator to measure distance and RSS in each possible direction when he needs to select the path, and then determine the ahead direction based on the comparison of distance and RSS.

Fig. 1. An in-building fire rescue scenario.

direction based on the comparison of distances and RSS. Since barometer is able to measure sufficiently accurate relative height information [14], orientation, i.e., direction finding, is a key issue that needs to be addressed in relative positioning works.

General direction finding technologies, such as radar [15] and geomagnetic-based method [16], are susceptible to surrounding conditions, or need to set up a fingerprint database, which may not be feasible in the rescue applications. Above all, existing positioning or direction finding technologies are difficult to meet the special needs of emergency search and rescue. Thus, we propose a template-matching-based orientation method. In comparison with traditional positioning technologies, it does not need to deploy the infrastructure in advance and also shows better orientation accuracy, which is more suitable for emergency rescue applications. Moreover, it is not limited by the surroundings conditions, and not need to make any software setup in advance, which is more convenient than traditional direction finding methods.

When the searcher needs to judge the moving path or direction, he should stand still and hold our proposed locator, which is composed of an Ultra Wideband (UWB) [17] chip to measure the distance, and a digital compass [18] to measure the rotation angle. The searcher spins around himself and measures the distance between the trapped and himself. Then a measurement sequence, consisting of distance values and angle values, is obtained. The detailed work-flow will be described in Section 2. Theoretically, to determine the relative direction to the trapped, we only need to find the rotation angle in corresponding to the minimum distance.

However, when the searcher rotates the locator, there is a certain region where the human body blocks the UWB signal transmission between the rotating locator and the target locator, which could introduce large ranging errors. Thus, it is not reliable to determine the direction by the minimum ranging value alone. In order to solve this problem, we introduce template matching method to take the whole measurement sequence into account. In literature [19], template matching is applied to the acoustic signal recognition. It describes a system that detects onsets of the bass drum, snare drum, and hi-hat cymbals in polyphonic audio signals of popular songs, which is based on a template-matching method that uses power spectrograms of drum sounds as templates.

With use of template matching method, we firstly need to establish a standard template and compare it with the measuring sequence, and finally obtain the optimal result which fits best with the standard template. In this paper, by measuring the distance and angle sequences as input signals, as long as a precise standard matching template is established, the relative direction between the searcher and the trapped could be obtained by our proposed template matching algorithm.

To construct a more accurate standard template, we should take the human body occlusion factor into account, with considering its impacts on the ranging accuracy. Although the IEEE802.15.4A standard provides some multi-path channel models, they do not take the influence of the human body into account. However, to the best of our knowledge, existing TOA ranging error models do not mention the influence of human body. Thus, in this paper, we establish a human occlusion error model to quantize the influence of human occlusion on the signal ranging.

The main contributions of this paper are as follows:

- We combined template matching with indoor positioning and proposed a template-matching-based orientation algorithm (TMOA). It could determine the relative direction effectively instead of finding the absolute coordinate, which is more suitable for emergency rescue applications.
- We defined Occlusion Sector and established a human occlusion error model (HOEM). It serves as the basis of establishment of the standard template.
- We optimized the matching process by dividing the matching process into two phase: Global Matching and Local Matching. It greatly improves the accuracy of the matching algorithm.

The rest of this paper is organized as follows. Section 2 fully explains the key issues that need to be solved in this paper. The occlusion sector is defined and the original template is established. Section 3 establishes a human body occlusion error model by fitting under various test conditions. Section 4 describes the specific process of TMOA based on HOEM. Section 5 builds a measurement system. The HOEM is verified and the we compare the TMOA with other traditional matching algorithm to verify the high efficiency and reliability. Section 6 summarizes the paper.

2. Problem description

2.1. Definition of application scenarios

For better description of the rescue procedure presented in Fig. 1, we further illustrate how the searcher operates the locator

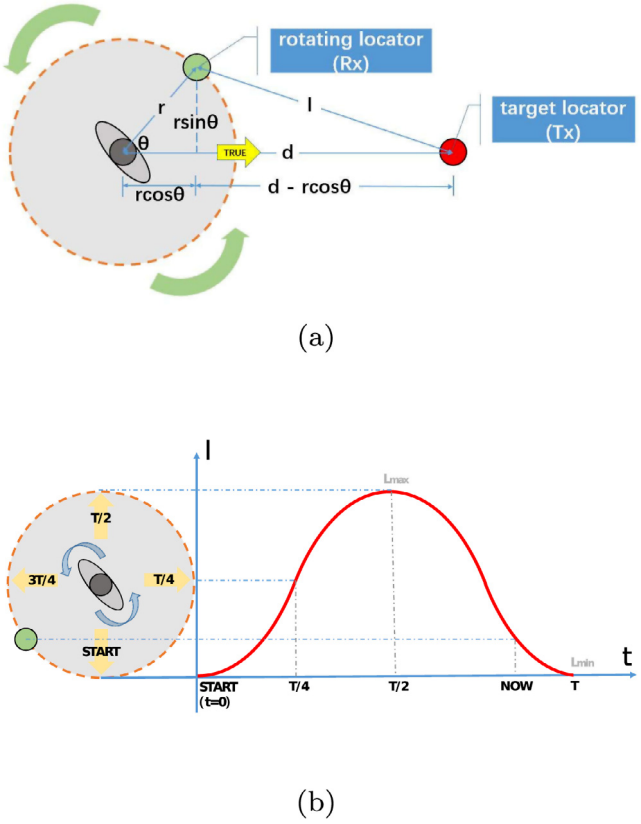

Fig. 2. Definition of application scenarios: (a) The geometric representation of rotational orientation scenario at a moment; (b) The process of obtaining the whole measurement sequence.

to localize the trapped. Since the searcher needs rotate with the locator, the rotational orientation scenario is described as the geometric relationship as shown in Fig. 2-(a). Target locator (denoted as Tx) and rotating locator (denoted as Rx) respectively refer to the devices mounted onto the trapped and searcher.

The searcher's orientation towards the Tx is denoted as θ_{true}, which is exactly the direction we need to determine. As the searcher spins around, radius of the circle rotation is denoted as r, the arm length of searcher. The direct distance between the searcher and the trapped is denoted as d. The angle between θ_{true} and the searcher's orientation while rotating is denoted as θ.

The measured distance between Tx and Rx is l. Thus, the direct distance between Tx and Rx could be derived as

$$d = l_{min} + r \tag{1}$$

where l_{min} is the minimum of the measured distance sequence, and r could be easily obtained by practical measurement.

Definition 1 (*Original Template*)**.** The relationship between l and θ, which could be seen from Fig. 2-(a), is described as follows:

$$\begin{aligned} l(\theta) &= \sqrt{(d - r\cos\theta)^2 + (r\sin\theta)^2} \\ &= \sqrt{r^2 + d^2 - 2dr\cos\theta} \end{aligned} \tag{2}$$

When the searcher spins around, Rx simultaneously measures the distance l and the angle θ at time t, denoted as a tuple (l_t, θ_t). Thus, as shown in Fig. 2-(b), the whole measurement sequence could be denoted as $S = \{(l_1, \theta_1), (l_2, \theta_2), \ldots, (l_n, \theta_n)\}$, where n corresponds to the sampling time. Theoretically, the expected result of θ_{true} could be obtained by the angle value corresponding to l_{min}. However, practical distance measuring could be affected by non-line-of-sight (NLOS) and multi-path factors [20], mainly caused by human body occlusion. Thus, we proposed a template-matching based orientation algorithm to calculate θ_{true} with building a human occlusion error model.

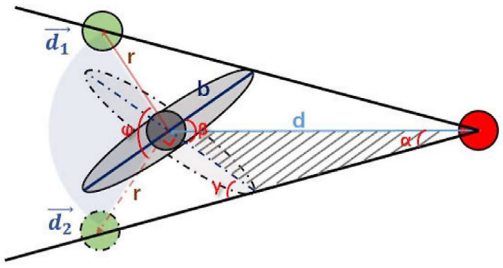

Fig. 3. The Occlusion Sector.

2.2. Occlusion sector

Definition 2 (*Occlusion Sector*)**.** As shown in Fig. 3 detailed, during the rotating process, there is a certain region where the searcher's body blocks the signal between Tx and Rx. We define this region as *Occlusion Sector*.

The width of the human body is denoted as b. It could be seen from Fig. 3 that signal is occluded when the searcher's orientation is between $\vec{d_1}$ and $\vec{d_2}$. Signal strength observed in this sector will be apparently lower. Thus, the sector between $\vec{d_1}$ and $\vec{d_2}$ is exactly the Occlusion Sector, whose angle is denoted as ϕ. According to law of sines [21], we could easily get $\frac{b/2}{\sin\alpha} = \frac{d}{\sin(180°-\gamma)}$, i.e., $\frac{b}{2\sin\alpha} = \frac{d}{\sin\gamma}$. Furthermore, as shown in Fig. 3, we could get

$$\begin{cases} \gamma = \alpha + \dfrac{\beta}{2} \\ \gamma = arctan\dfrac{r}{b/2} \\ \phi = 180° - \beta \end{cases} \tag{3}$$

thus ϕ could be derived as

$$\phi = 180° - 2(arctan\frac{2r}{b} - arcsin\frac{br}{d\sqrt{4r^2 + b^2}}) \tag{4}$$

Since the width of human body b is approximately equal to 0.4 m, as well as $b \ll d$, $r \ll d$ and $b \approx 2r$, we could conclude that

$$\phi = 180° - 2arctan\frac{2r}{b} \approx 90° \tag{5}$$

2.3. The standard template

Definition 3 (*Standard Template*)**.** With considering the human body occlusion error, we improved the original template mentioned above, which we call *standard template*, described as follows:

$$l(\theta) = \begin{cases} \sqrt{r^2 + d^2 - 2dr\cos\theta} + \varepsilon_{on-body}, & 135° \le \theta \le 225° \\ \sqrt{r^2 + d^2 - 2dr\cos\theta}, & others \end{cases} \tag{6}$$

where $\varepsilon_{on-body}$ is the human body occlusion error.

Next, we will quantify $\varepsilon_{on-body}$ by means of practical measurement modeling, which will be detailed in Section 3.

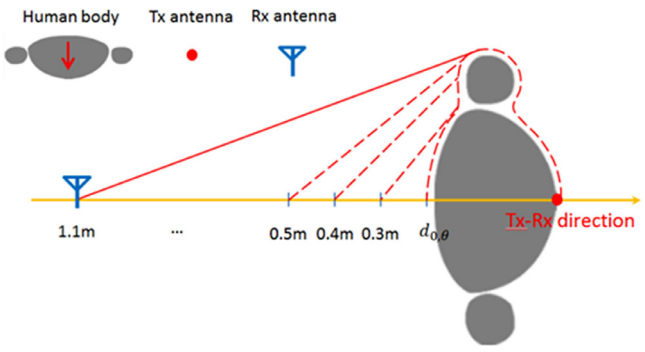

Fig. 4. The propagation of ranging signals in human occlusion scenarios.

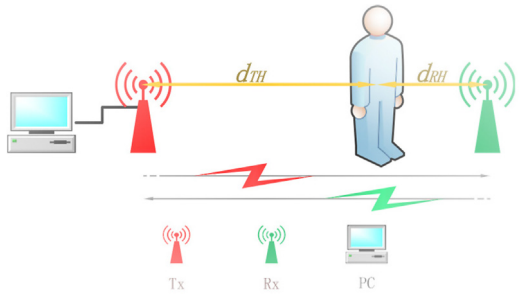

Fig. 5. The system for measuring the ranging distance.

3. HOEM: Human occlusion error model

As shown in Fig. 4, the ranging signal is emitted by Tx, then creeps from one side to the other side along the human body, and finally reaches Rx by propagating in the air. Many factors, such as blocking, creeping waves [22] and multi-path [23], have impact on ranging accuracy. When the distance between Tx and human varies, the main factor affecting ranging is different. If Tx is far away from the human body, the attenuation could mainly comes from multi-path and the path loss caused by the air propagation possibly [24]. If Tx is close to the human body, blocking and creeping waves are possibly the main factors. Thus, there could be a threshold of distance which determines the main factors affecting $\varepsilon_{on-body}$.

3.1. Experiment setting

As shown in Fig. 5, the system for measuring the ranging distance consists mainly of a set of ranging locators (Tx and Rx) and a laptop. The scenario is an outdoor environment and there is no occlusion of large buildings or trees around. The experimenter stands still between Tx and Rx. Place the antennas on tripods to ensure the consistency of vertical height.

A measuring case is represented as follows:

$$Case = (d_{TH}, d_{RH}) \tag{7}$$

where d_{TH} is the distance between Tx and the human surface and d_{RH} is the distance between Rx and the human surface. For each case, the distance measurement error is modeled with d_{TH} and d_{RH}. The setting of *Case* as shown in Table 1. d_{TH} varies from 0 m to 1.8 m increasing by 0.1 m at a time, and d_{RH} is 0 m, 0.2 m, 0.3 m, and 0.5 m in different cases. To ensure the validity of the result, we perform 500 ranging items under each *Case* setting.

Table 1
Setting of variables for human body occlusion scenario.

d_{TH} (m)	d_{RH} (m)
(0, 0.1, 0.2, 0.3, 0.4, 0.5, 0.6, 0.7, 0.8, 0.9, 1, 1.1, 1.2, 1.3, 1.4, 1.5, 1.6, 1.7, 1.8)	(0, 0.2, 0.3, 0.5)

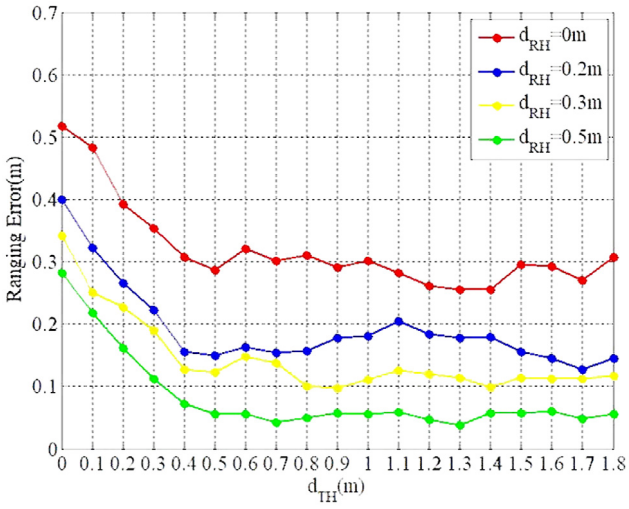

Fig. 6. The general characteristics of ranging error distribution.

3.2. General characteristics of ranging errors

As shown in Fig. 6, the general characteristics of ranging error distribution is obtained under different cases. When d_{RH} is determined, the variation trend of ranging error varies when d_{TH} is smaller or larger than 0.5 m. The ranging error decreases as the d_{TH} increases when d_{TH} is smaller than 0.5 m, which is possibly because the signal is mainly affected by the surface creeping wave. There is only a small fluctuation when d_{TH} is larger than 0.5 m, which is possibly because that the signal is mainly affected by the attenuation propagating in the air. Thus, we could generally conclude that 0.5 m is the threshold mentioned above.

Definition 4 (*Body-Surface-Area*)**.** When d_{TH} is smaller than the threshold 0.5 m, the region is called *Body-Surface-Area*.

Definition 5 (*Non-Body-Surface-Area*)**.** When d_{TH} is larger than the threshold 0.5 m, the region is called *Non-Body-Surface-Area*.

3.3. Modeling the ranging error

In common sense, the arm length is usually less than 0.5 m. Thus, in this paper, we only take the TOA ranging error modeling in the Body-Surface-Area into consideration. When the distance between the antenna and the human body is d_{TH}, the TOA ranging error $ERR_{d_{TH}}$ could be formulated as:

$$ERR_{d_{TH}} = ERR_{d_{TH}-d_{RH}} - ERR_{(d_{TH}=0.5)\cap d_{RH}} \tag{8}$$

where $ERR_{d_{TH}-d_{RH}}$ is the TOA ranging error between Tx and Rx, and $ERR_{(d_{TH}=0.5)\cap d_{RH}}$ is the TOA ranging error between Tx and Rx if d_{TH} is 0.5 m.

Typical distribution results of the ranging error as shown in Fig. 7. It could be easily seen that all the ranging errors obey Gaussian distribution. The TOA ranging error of the Body-Surface-Area $\varepsilon_{on-body}$ could be modeled as follows:

$$\varepsilon_{on-body} = N(\mu_{on-body}, \sigma_{on-body}) \tag{9}$$

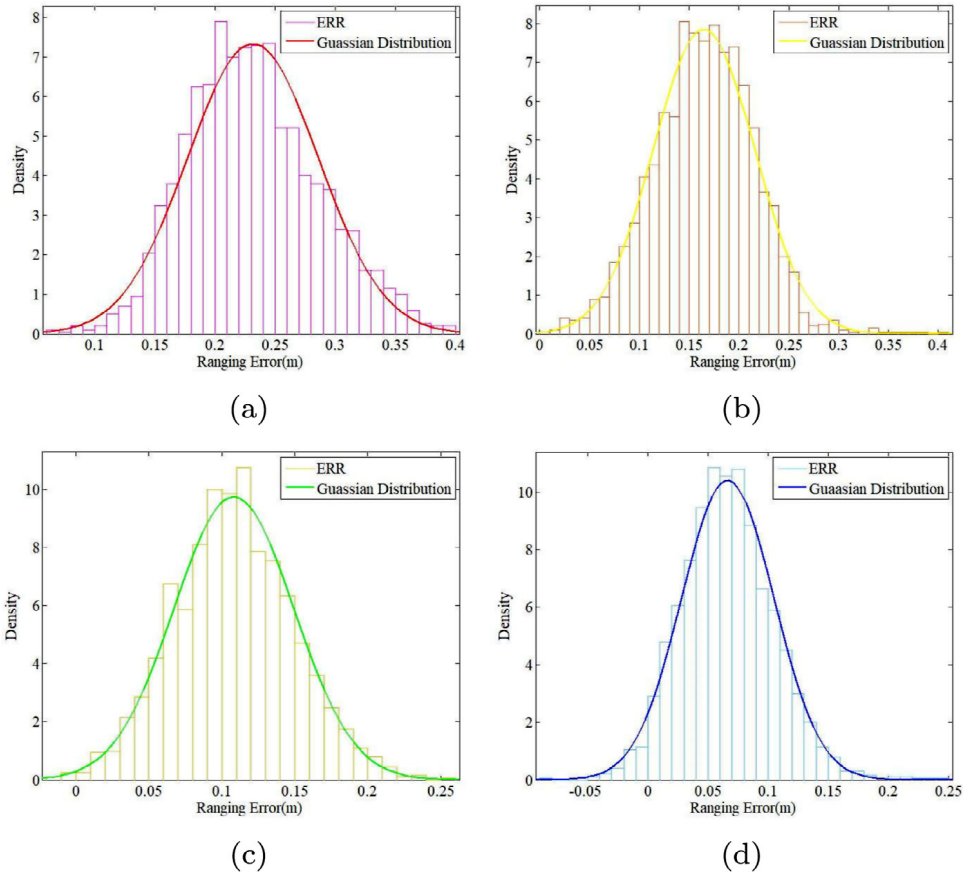

Fig. 7. Typical distribution results of the ranging error: (a) $d_{TH} = 0$ m; (b) $d_{TH} = 0.1$ m; (c) $d_{TH} = 0.2$ m; (d) $d_{TH} = 0.3$ m.

Table 2
The $\mu_{on-body}$ and the $\sigma_{on-body}$ of ranging error in the Body-Surface-Area.

d_{TH} (m)	$\mu_{on-body}$	$\sigma_{on-body}$
0	0.2316	0.0544
0.1	0.1648	0.0508
0.2	0.1082	0.0409
0.3	0.0665	0.0383
0.4	0.0122	0.0371

where $\mu_{on-body}$ is the mean of $\varepsilon_{on-body}$, and $\sigma_{on-body}$ is the standard deviation of $\varepsilon_{on-body}$.

The value of $\mu_{on-body}$ and $\sigma_{on-body}$ under different condition as shown in Table 2. Fit $\mu_{on-body}$ and $\sigma_{on-body}$ separately by least squares method. Fig. 8-(a) and -(b) show the fitting results of $\mu_{on-body}$ and $\sigma_{on-body}$, respectively.

We could deduce the HOEM according the fitting result:

$$\mu_{on-body} = -0.5371 \times d_{TH} + 0.2241 \tag{10}$$

$$\sigma_{on-body} = -0.0471 \times d_{TH} + 0.0537 \tag{11}$$

4. TMOA: Template-matching-based orientation algorithm

With considering HOEM, we could achieve an improved standard template. In order to obtain the θ_{true}, the measurement sequence $S = \{(l_1, \theta_1), (l_2, \theta_2), \ldots, (l_n, \theta_n)\}$ needs to be matched with the standard template.

The standard template is n-divided to obtain a standard template sequence. In order to obtain a more accurate matching result, we divided the standard template into n equal parts. Then, the matching process are divided into two phases: (1) *Global Matching*: Firstly the measurement sequence is matched with the standard template, then we could obtain a preliminary estimation θ_{first}; (2) *Local Matching*: Select a sequence segment from the measurement sequence centering on θ_{first}. Then, we perform the matching process again with the standard template. Finally, the expected matching result θ_{true} could be achieved.

4.1. Global matching

Fig. 9 shows the process of Global Matching. The green is the standard template sequence and the red is the measurement sequence. Seq-Euclidean [25] between the measurement and the standard template sequence is viewed as the matching similarity criterion.

Definition 6 (*Seq-Euclidean*)**.** The *Seq-Euclidean* is a criterion to determine the similarity of two sequence. The smaller the Seq-Euclidean, the higher the similarity. For better to describe the Seq-Euclidean, we denoted a time sequence as $T = \{t_1, t_2, \ldots, t_n\}$. Sequences $A = \{a_1, a_2, \ldots, a_n\}$ and Sequences $B = \{b_1, b_2, \ldots, b_n\}$ are both generated with T. Thus, the Seq-Euclidean d_{A_B} of A and B is denoted as:

$$d_{A\_B} = \sum_{i=1}^{n} \sqrt{(a_i - b_i)^2} \tag{12}$$

The process of Global Matching is as follows:

Step 1: The measurement sequence remains static. The standard template sequence moves rightward step by step with an interval of the rotation angle, starting from t_0.

Step 2: The Seq-Euclidean between the two sequences is calculated in each step.

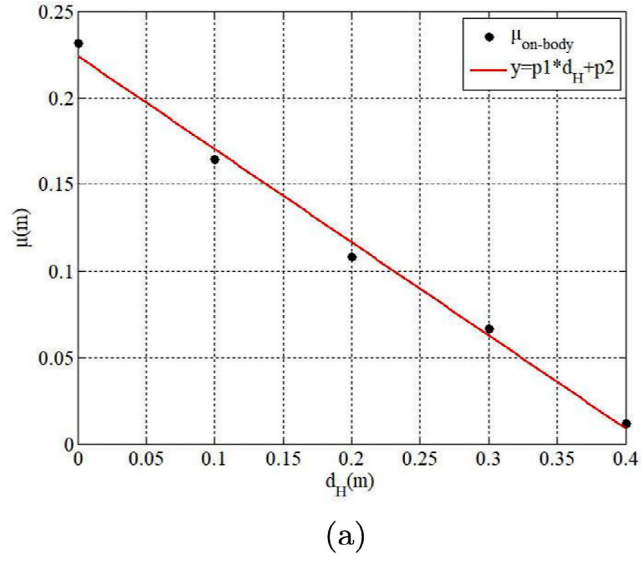

Fig. 8. The fitting result: (a) $\mu_{on-body}$; (b) $\sigma_{on-body}$.

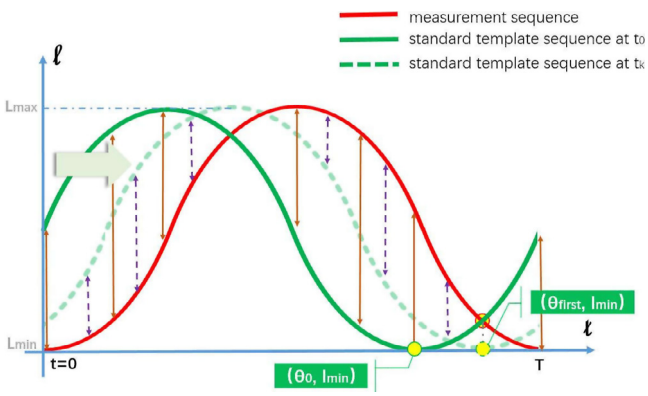

Fig. 9. Process of global matching. (For interpretation of the references to color in this figure legend, the reader is referred to the web version of this article.)

Step 3: Find the moment t_k when the Seq-Euclidean is minimum, and locate the position of (θ_0, l_{min}) in the standard template sequence at t_k, as shown in Fig. 9.

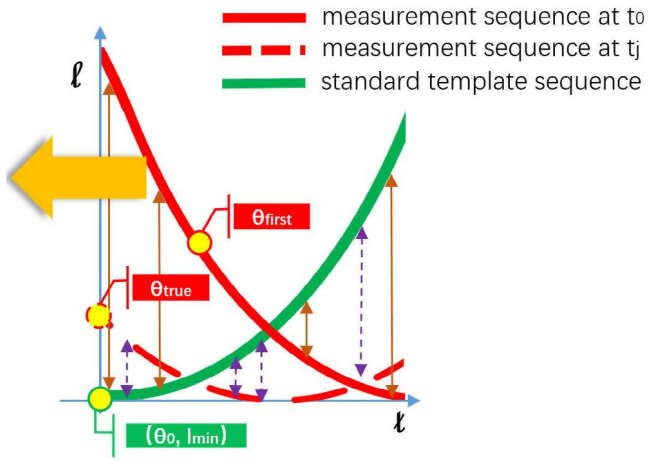

Fig. 10. Process of local matching. (For interpretation of the references to color in this figure legend, the reader is referred to the web version of this article.)

Step 4: In correspondence to (θ_0, l_{min}), the preliminary estimation θ_{first} could be obtained.

4.2. Local matching

Fig. 10 shows the process of Local Matching. The green is the standard template sequence segment and the red is the measurement sequence segment.

The process of Local Matching is as follows:

Step 1: Centering on θ_{first}, take p items respectively from left and right sides of the measurement sequence as a segment.

Step 2: Take q items out of the standard sequence as a segment, starting from (θ_0, l_{min}).

Step 3: The standard template sequence segment remains static. The measurement sequence segment moves leftward step by step with an interval of the rotation angle, starting from t_0.

Step 4: The new Seq-Euclidean between the two sequences is calculated in each step.

Step 5: Find the moment t_j when the Seq-Euclidean is minimum.

Step 6: The expected matching result θ_{true} could be obtained according to the position of (θ_0, l_{min}), as shown in Fig. 10.

For better illustrate the process of proposed matching algorithm, pseudo code is displayed in Algorithm 1. To determine the preliminary estimation during the process of Global Matching, the computational cost mainly comes from computing the Seq-Euclidean. The computational complexity is $O(N^2)$. To determine the expected matching result during the process of Local Matching, the computational cost also mainly comes from computing the Seq-Euclidean and the computational complexity is $O(N^2)$. So the computational complexity of TMOA is $O(N^2)$.

5. Experiment system

In order to verify our proposed model and algorithm, we set up a practical measuring system, as shown in Fig. 11, and verify HOEM and TMOA respectively in field tests. Our own-designed system mainly consists of two locators, namely Tx and Rx. Tx is equipped on the trapped and Rx on the searcher. Both of them are composed of MCU, a TOA module and a digital compass.

The MCU module is based on the stm32f103 chip [26]. It provides serial port function, debugging function, power management function, SPI communication function, and includes USB2.0OTG full-speed interface.

Algorithm 1 TMOA based on HOEM

Input: : The measurement sequence S and the standard template sequence T (both two sequences consist of l (the distance between Tx and Rx) and θ (the angle between the searcher's orientation towards the Tx and the searcher's orientation while rotating). The notation $S.l$ stands for l of the measurement sequence and $T.l$ stands for l of the standard template sequence); the rotation radius r; initialized p, q and ψ;

Output: : The relative direction θ_{true}.

$\psi = 0$
Global Matching
for $index = 0$ to $n - 1$ **do**
  for $i = 0$ to $n - 1$ **do**
    $\psi^2 = (\psi + (S.l[i] - T.l[i + index])^2)^2$
  end for
  $distanceGlobal[index] = \psi$
end for
if $distanceGlobal[index] < Dist_{min}$ **then**
  $Dist_{min} = distanceGlobal[index]$
  $Index_{min} = index$
end if
$\psi = 0$
Local Matching
for $index = (Index_{min} - p)$ to $(Index_{min} + p)$ **do**
  for $j = 0$ to $q - 1$ **do**
    $\psi^2 = (\psi + (S.l[j + index] - T.l[j])^2)^2$
  end for
  $distanceLocal[index] = \psi$
end for
if $distanceLocal[index] < Dist_{min}$ **then**
  $Dist_{min} = distanceLocal[index]$
  $Index_{result} = index$
end if
$\theta_{true} = S.\theta[Index_{result}]$

The TOA module uses the DW1000 chip [27]. The DW1000 is a sensor based on ultra-widescreen technology launched by DecaWave, which is a single-chip wireless transceiver chip. The DW1000 supports 6 frequency bands with the center band between 3.5 GHz and 6.5 GHz. The transmitted power ranges from −14 dbm to −10 dbm, and the integrated antenna enables users to transmit signals directly through the antenna. The DW1000 has powerful anti-interference ability for multi-path weakening.

The type of digital compass model is DCM260B [28], which is a three-dimensional digital compass with high-precision. It uses hard magnetic and soft magnetic calibration algorithms to get more accurate result even in magnetic field. It is small size, low power consumption, high shock resistance and high reliability, etc., which enables it to work normally even in harsh environments. It is also suitable for high-precision measurement integrated control system.

For verifying the validity of HOEM, representative measurement results are compared with model generating results. Firstly, We measured and calculated TOA ranging errors of 500 groups when d_{RH} is 0.5 m and d_{TH} is from 0 m to 0.5 m by step 0.1 m in the same human occlusion scenario. Then the TOA ranging error simulated data of d_{TH} between 0 m and 0.5 m under the same condition are obtained by simulated with MATLAB software.

In order to verify the superiority of TMOA using HOEM, we compared the algorithm with two typical template-matching algorithms, namely correlation coefficient [29] and matching filter [30]. All three matching algorithms are compared in two conditions: with or without taking HOEM into consideration. The parameters p and q needed for Local Matching of TMOA are respectively set as 40 and 4.

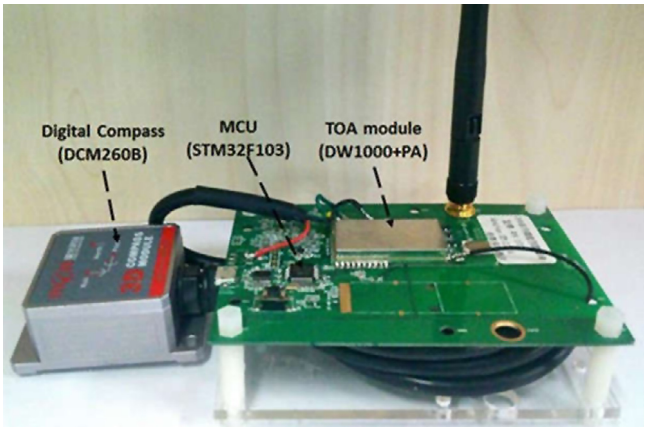

Fig. 11. The practical measuring system.

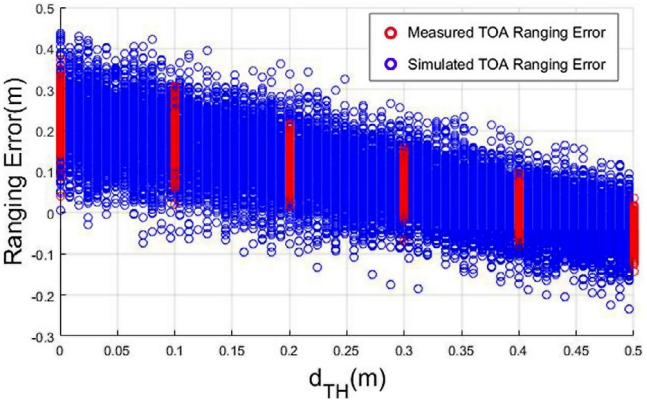

Fig. 12. Verification for HOEM: the comparison between the measured data and the simulated data.

6. Results and discussion

6.1. Verification for HOEM

Fig. 12 shows the comparison between the measured data and the simulated data. It could be seen that the measured data has very high similarity with the simulated data. It shows that HOEM has certain credibility. Since the general characteristics of ranging error distribution is obtained under different cases in Section 3, we could generally conclude that 0.5 m is the threshold. In common sense, the arm length is less than 0.5 m. Thus, in this paper, we only take the TOA ranging error modeling in the Body-Surface-Area into consideration.

If Tx is far away from the human body, the attenuation could mainly comes from multi-path and the path loss caused by the air propagation possibly. If Tx is close to the human body, blocking and creeping waves are possibly the main factors. As shown in Fig. 12, when the distance between antenna and human body is less than or equal to 0.5 m, i.e., when the antenna is placed in the Body-Surface-Area, the TOA ranging error decreases with the increase of the distance between antenna and human body, and the fluctuation amplitude decreases, since the effects of blocking and creeping waves decreases.

6.2. Verification for TMOA

Fig. 13 is cumulative-probability distribution function (CDF) of estimation error with considering above-mentioned three matching algorithms. As shown in Fig. 13, the maximum angle error of

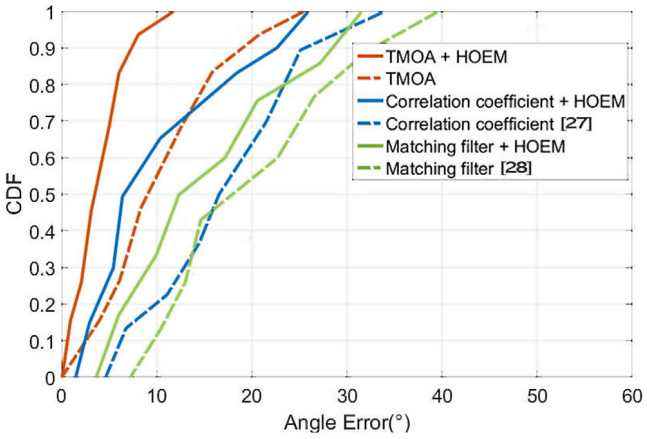

Fig. 13. Verification for TMOA: CDF estimation error of three matching algorithms.

TMOA is 25 degrees, while correlation coefficient is 33 degrees and matching filter is 40 degrees; the average angle error of TMOA is 9 degrees, while correlation coefficient is 16 degrees and matching filter is 18 degrees. Furthermore, the maximum angle error of TMOA improved by HOEM is 12 degrees, while correlation coefficient improved by HOEM is 25 degrees and matching filter is 32 degrees; the average angle error of TMOA improved by HOEM is 4 degrees, while correlation coefficient improved by HOEM is 7 degrees and matching filter improved by HOEM is 12 degrees.

As can be seen from the figure, for all these three matching algorithms, the accuracy could be greatly improved with considering HOEM, since we take the human body occlusion factor into account and improve the ranging accuracy. Under the same condition, more accurate results could be achieved with the use of TMOA and HOEM, than the other two comparing algorithms, since we optimized the matching process by dividing the matching process into two phase: Global Matching and Local Matching. It greatly improves the accuracy of the matching algorithm.

7. Conclusions

In this paper, we proposed a new orientation algorithm based on template matching for emergency rescue scenarios. It barely need to deploy any infrastructure in advance to obtain the relative positional relationship between the searcher and the trapped effectively. Furthermore, it is insusceptible to surrounding conditions and undesired to set up a fingerprint database, which may is more convenient in the rescue applications. In order to improve the accuracy of orientation, we proposed two basic methods. Firstly we considered the effects of human body occlusion and established a ranging error model (HOEM). Then we proposed a template-matching-based algorithm (TMOA) and divided the matching process into two phases: Global Matching and Local Matching. Experiment shows that result of TMOA is more accurate than other two typical template-matching algorithm under the same condition. With the application of HOEM and TOMA, the problem of indoor positioning in emergency rescue in complex building environment could be solved better. Although it can work better than traditional positioning or direction finding technologies, the searcher still faces to a strict operation procedure. The searching process needs to be more automated and less manual, which could greatly improve rescue efficiency. This implies our future research directions.

Declaration of competing interest

The authors declare that they have no known competing financial interests or personal relationships that could have appeared to influence the work reported in this paper.

Acknowledgments

This work is supported in part by the National Key R&D Program of China under Grant 2016YFB0700500, and in part by the National Postdoctoral Program for Innovative Talents, China under Grant BX20190033, and in part by the Fundamental Research Funds for the Central Universities, China under Grant 06500127, and in part by National Natural Science Foundation of China (NSFC) project No. 61671056. The authors would like to thank Jiahui Lv, Yanzhong Liu, Yanan Wu, and Liyuan Xu for their fundamental work in this paper.

Appendix A. Supplementary data

Supplementary material related to this article can be found online at https://doi.org/10.1016/j.phycom.2019.100910.

References

[1] L. Yu, Y. Liu, T. Chi, et al., An IBeacon-based indoor and outdoor positioning system for the fire emergency command, 2017 Forum on Cooperative Positioning and Service (CPGPS), IEEE, 2017, pp. 326–329.
[2] Nguyen-Son Vo, Antonino Masaracchia, Long D. Nguyen, Ba-Cuong Huynh, Natural disaster and environmental monitoring system for smart cities: Design and installation insights, EAI Endorsed Trans. Ind. Netw. Intell. Syst. 5 (16) (2018) 1–9.
[3] Long D. Nguyen, Ayse Kortun, Trung Q. Duong, An introduction of real-time embedded optimisation programming for UAV systems under disaster communication, EAI Endorsed Trans. Ind. Netw. Intell. Syst. 5 (17) (2018).
[4] B. Jang, H. Kim, Indoor positioning technologies without offline fingerprinting map: A survey, in: IEEE Communications Surveys & Tutorials, 2019.
[5] F. Zafari, A. Gkelias, K.K. Leung, A survey of indoor localization systems and technologies, in: IEEE Communications Surveys & Tutorials, 2019.
[6] A. Achroufene, Y. Amirat, A. Chibani, RSS-based indoor localization using belief function theory, IEEE Trans. Autom. Sci. Eng. (2018).
[7] X. Zhu, W. Zhu, Z. Chen, Direct localization based on motion analysis of single-station using TOA, in: 2018 2nd IEEE Advanced Information Management, Communicates, Electronic and Automation Control Conference (IMCEC), IEEE, 2018, pp. 1823–1827.
[8] G. Fokin, A. Kireev, A.H.A. Al-odhari, TDOA positioning accuracy performance evaluation for arc sensor configuration, in: 2018 Systems of Signals Generating and Processing in the Field of on Board Communications, IEEE, 2018, pp. 1–5.
[9] L. Yu, Y. Liu, T. Chi, et al., An iBeacon-based indoor and outdoor positioning system for the fire emergency command, in: 2017 Forum on Cooperative Positioning and Service (CPGPS), IEEE, 2017, pp. 326–329.
[10] W. Zhang, M.I.S. Chowdhury, M. Kavehrad, Asynchronous indoor positioning system based on visible light communications, Opt. Eng. 53 (4) (2014) 045105.
[11] N.C. Yadav, A. Shanmukha, B.M. Amruth, Development of GPS/INS integration module using Kalman filter, in: 2017 International Conference on Algorithms, Methodology, Models and Applications in Emerging Technologies (ICAMMAET), IEEE, 2017, pp. 1–5.
[12] X. Nong, L. Cheng, D. Yating, et al., Research on indoor navigation of mobile robot based on INS and ultrosound, in: 2017 12th IEEE Conference on Industrial Electronics and Applications (ICIEA), IEEE, 2017, pp. 231–235.
[13] P. Wang, J. He, L. Xu, et al., Characteristic modeling of TOA ranging error in rotating anchor-based relative positioning, IEEE Sens. J. 17 (23) (2017) 7945–7953.
[14] Y. Son, S. Oh, A barometer-IMU fusion method for vertical velocity and height estimation, in: 2015 IEEE Sensors, IEEE, 2015, pp. 1–4.
[15] D. Wang, Q. Bao, R. Tian, et al., Bistatic weak target detection method using non-cooperative air surveillance radar, J. Syst. Eng. Electron. 26 (5) (2015) 954–963.
[16] T. Otsuyama, J. Honda, A study of direction finding method for passive airport surveillance radar, in: 2014 International Symposium on Antennas and Propagation Conference Proceedings, IEEE, 2014, pp. 393–394.

[17] A.A. Ibrahim, Compact planer UWB antenna for high speed communications, in: 2019 International Conference on Innovative Trends in Computer Engineering (ITCE), IEEE, 2019, pp. 266–269.
[18] V.X. Hau, V.E. Ivanov, Results of the development and experimental studies of the digital magnetic compass system, in: 2018 Ural Symposium on Biomedical Engineering, Radioelectronics and Information Technology (USBEREIT), IEEE, 2018, pp. 359–362.
[19] K. Yoshii, M. Goto, H.G. Okuno, Drum sound recognition for polyphonic audio signals by adaptation and matching of spectrogram templates with harmonic structure suppression, IEEE Trans. Audio Speech Lang. Process. 15 (1) (2006) 333–345.
[20] S. Wu, S. Zhang, D. Huang, A TOA-based localization algorithm with simultaneous NLOS mitigation and synchronization error elimination, IEEE Sensors Letters 3 (3) (2019) 1–4.
[21] M.G. Arnold, Approximating trigonometric functions with the laws of sines and cosines using the logarithmic number system, in: 8th Euromicro Conference on Digital System Design (DSD'05), IEEE, 2005, pp. 48–53.
[22] D.B. Smith, D. Miniutti, T.A. Lamahewa, et al., Propagation models for body-area networks: A survey and new outlook, IEEE Antennas Propag. Mag. 55 (5) (2013) 97–117.
[23] W. Xiuzhen, H. Yanyan, L. Sanrong, Fast positioning scheme for UWB in the multi-path environment, in: 2016 8th IEEE International Conference on Communication Software and Networks (ICCSN), IEEE, 2016, pp. 530–534.
[24] S. Zhang, G.F. Pedersen, Mutual coupling reduction for UWB MIMO antennas with a wideband neutralization line, IEEE Antennas Wirel. Propag. Lett. 15 (2016) 166–169.
[25] M.D. Malkauthekar, Analysis of Euclidean distance and Manhattan distance measure in Face recognition, 2013.
[26] STM32F103 datasheet, 2019, Available online: https://www.st.com/en (accessed on 1 April 2019).
[27] Y. Li, Y. Li, Z. Polytechnic, Design and optimization of indoor positioning system based on DW1000, Wirel. Internet Technol. (2016).
[28] DCM260B compass, 2019, Available online: http://www.rion-electronic.com (accessed on 9 April 2019).
[29] R. Sudha, V. Ragavi, C. Thirumalai, Analyzing correlation coefficient using software metrics, in: 2017 International Conference on Trends in Electronics and Informatics (ICEI), IEEE, 2017, pp. 1151–1153.
[30] S. Chen, C. Luo, H. Wang, et al., Matched filtering and orthogonal matching pursuit for terahertz coded-aperture imaging, in: 2018 5th International Conference on Information, Cybernetics, and Computational Social Systems (ICCSS), IEEE, 2018, pp. 102–104.

Jiawang Wan received the B.E. degree from the University of Science and Technology Beijing, China, in 2017, and he is currently working towards the Ph.D degree at University of Science and Technology Beijing. His research interests include wireless localization, swarm intelligence and Internet of things.

Cheng Xu received the B.E., M.E. and Ph.D degrees from the University of Science and Technology Beijing, China, in 2012, 2015 and 2019, respectively, where he is currently working as an Assistant Professor at University of Science and Technology Beijing. His research interests include wireless localization, swarm intelligence and Internet of things.

Xiaotong Zhang received the M.S., and Ph.D. degrees from University of Science and Technology Beijing , in 1997, and 2000, respectively. He was a Professor in the Department of Computer Science and Technology, University of Science and Technology Beijing. His research includes work in quality of wireless channels and networks, wireless sensor networks, networks management, cross-layer design and resource allocation of broadband and wireless network, signal processing of communication and computer architecture.

Jie He received the B.E. and Ph.D. degrees from the University of Science and Technology Beijing, Beijing, China, in 2005 and 2012, respectively, where he is an Associate Professor. His current research interests include indoor location system, wireless sensor networks, and body area network.

Shihong Duan received Ph.D. degree in computer science from University of Science and Technology Beijing. She is an associate professor with the School of Computer and Communication Engineering, USTB . Her research interests includes wireless indoor positioning, human gesture recognition and motion capture.